ISBN: 978-3-95450-208-0 doi:10.18429/JACoW-IPAC2019-WEPGW096

DEVELOPMENT OF SUPERSONIC GAS-SHEET-BASED BEAM PROFILE MONITORS

H. D. Zhang†, A. Salehilashkajani, C. P. Welsch,
Cockcroft Institute and University of Liverpool, Warrington, UK
M. Ady, J. Glutting, O. R. Jones, T. Marriott-Dodington, S. Mazzoni, A. Rossi, G. Schneider,
R. Veness, CERN, Geneva, Switzerland
P. Forck, S. Udrea, GSI, Darmstadt, Germany

Abstract

Non-destructive beam profile monitoring is very desirable, essentially for any particle accelerator but particularly for high-energy and high-intensity machines. Supersonic gas jet-based monitors, detecting either the ionization or fluorescence of a gas sheet interacting with the primary beam to be characterized, allow for minimally invasive measurements. They can also be used over a wide energy range, from keV to TeV beams. This contribution gives an overview of the jet-based ionization and fluorescence beam profile monitors which have been developed, built and tested at the Cockcroft Institute. It discusses gas sheet generation, vacuum considerations, choice of gas species and detection methods.

INTRODUCTION

Beam diagnostics play a key role in the safe and reliable operation of any particle accelerator. Especially for high energy, high-intensity machines, it is of great importance that proper diagnostics with non-invasive methods are in place for continuous monitoring. Many methods can be used to determine the beam profile. Scintillating screens and SEM-Grids are used very frequently as invasive methods at proton accelerators. Synchrotron radiation provides a convenient and non-invasive means of beam imaging, but it is only applicable at the highest energy proton accelerators like LHC. Historically, ionisation beam profile monitoring (IPM) [1] or beam induced fluorescence (BIF) [1], based on the interaction between the primary beam and the residual gas, have been considered the least-invasive methods of measuring beam profiles in one dimension. Their application is often linked with specific locations where gas injection is allowed and a typically some meter-long pressure bump is acceptable; otherwise, a long integration time will be expected. Addressing these issues using IPM or BIF based on a supersonic gas jet curtain instead of the residual gas would be appropriate, since the gas jet curtain can be thin but with high density and can be pumped out easily because of its directionality. This contribution will discuss the development of such monitors based on experience of gas jet based IPM and BIF at the Cockcroft Institute (CI) in recent years.

MEASUREMENT PRINCIPLE

A supersonic gas jet curtain tilted at 45 degrees gets generated in the interaction chamber, with its direction perpendicular to that of the primary beam. The density of the gas jet is normally more than 10 times higher than the surrounding residual gas. In this way, the gas jet curtain resembles a scintillating screen, but is inconsumable. When the primary beam interacts with the gas jet curtain, ions, electrons and photons are generated. These can be collected to recover the profile information of the primary beam. Normally, the cross-section depends on the species of the jet and the energy and type of the primary beam. While IPM collects all the ions generated, BIF collects photons only in a certain solid angle. Hence BIF would require a much higher integration time than IPM to detect a primary beam, for the same gas jet density. A diagram illustrating this process can be seen in Fig. 1.

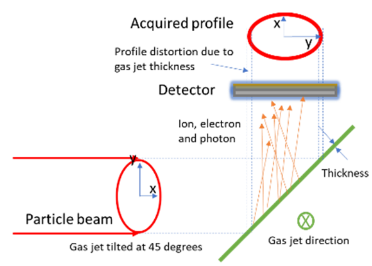

Figure 1: The principle of a gas-jet based beam profile monitor.

JET GENERATION AND MEASUREMENT

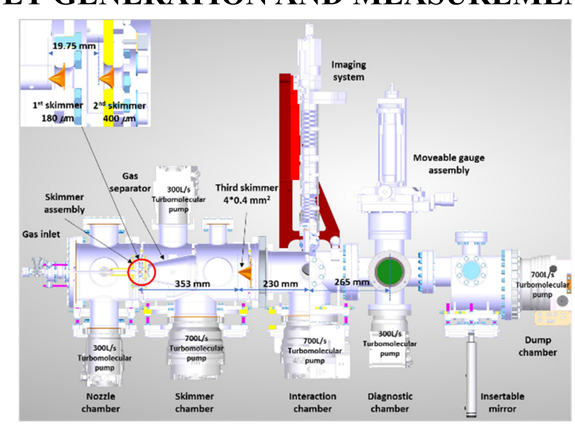

Figure 2: Schematic of a prototype gas-jet based beam profile monitor using BIF mode.

Using the setup at CI as an example, see Fig. 2, the supersonic gas jet must reach an equivalent pressure of 10^{-6}

† hao.zhang@cockcroft.ac.uk

ISBN: 978-3-95450-208-0 doi:10.18429/JACoW-IPAC2019-WEPGW096

mbar to make meaningful measurements with moderate exposure times. The supersonic gas jet is generated when a high-pressure gas expands through a 30 μm nozzle into a low-pressure region. In the nozzle chamber, the centreline density scales as the distance increases, which can be described ideally as Eq. 1[2] with the assumption of isentropic flow, ideal gas behaviour, constant heat capacity and continuum flow.

$$\rho = \frac{P_0}{k_B T_0}\left(1+\frac{\gamma-1}{2}M^2\right)^{-\frac{1}{\gamma-1}} \quad (1)$$

where γ is the heat capacity ratio and is ρ the number density, P_0 and T_0 are pressure and temperature at nozzle throat, and M is the Mach number which can be calculated using Eq. 2 [2].

$$M = A\left(\frac{x-x_0}{d}\right)^{\gamma-1} - \frac{\frac{1}{2}\left(\frac{\gamma+1}{\gamma-1}\right)}{A\left(\frac{x-x_0}{d}\right)^{\gamma-1}} \qquad \left(\frac{x}{d}\right) > \left(\frac{x}{d}\right)_{min} \quad (2)$$

Here d is the nozzle throat size, A and x_0 are fitted parameters which are γ-dependent as seen in Table 1.

Table 1: Centreline Mach Number for Axisymmetric Flow

γ	x_0/d	A	$(x/d)_{min}$
1.67	0.075	3.26	2.5
1.40	0.40	3.65	6

In reality, with the skimmer inserted and the stationary wall around the skimmer introduced, the density will decrease faster. A turbomolecular pump backing by a scroll pump is used to maintain a low pressure in the nozzle chamber, so that the gas jet generation process gets minimally disturbed by the surrounding gas. The choice of pumps depends on the mass flow and pressure to be maintained. The mass flow $\dot{m}$ can be calculated from Eq. 3 [3].

$$\dot{m} = P_0 A^* \sqrt{\frac{\gamma R T}{W}}\left(1+\frac{\gamma-1}{2}\right)^{-\frac{\gamma+1}{2(\gamma-1)}} \quad (3)$$

where A* is the nozzle throat area, R is the gas constant, W is the molecular mass.

To match the required density and divergence of a jet, a series of conical skimmers is used. With the help of differential pumping, the flow after the 1st skimmer may be considered to be molecular, therefore geometric expansion can be safely assumed. The final density ρ will decrease from the initial value $\rho_{skimmer}$ leaving the first skimmer with the transverse velocity spread v_{mean}/v_{jet} and distance from the skimmer x, according to Eq. 4 [2] and Eq. 5 [4].

$$v_{jet} = M\sqrt{\frac{\gamma R T_0}{W}}\left(1+\frac{\gamma-1}{2}M^2\right)^{-\frac{1}{2}} \quad (4)$$

$$\rho = \rho_{skimmer}\left(1+\frac{x * v_{mean}}{r_{skimmer} * v_{jet}}\right)^{-2} \quad (5)$$

It is obvious that careful skimmer positioning and sizing is key in reaching a given jet density and divergence. Note that these theoretical considerations are for guidance only, and accurate values should be validated by simulations and experiments. Here, the first and second skimmers have conical shapes with orifices of 180 μm and 400 μm. To allow for a 2D measurement of the beam profile, the last skimmer with a 4 × 0.4 mm2 slit opening will shape the jet into a curtain with a 45-degree tilt angle. The distances between the nozzle, each skimmer, and the interaction point are indicated in Fig. 2.

Turbomolecular pumps also should be installed at the chambers between all skimmers, to create differential pumping stages and ensure that molecules collimated off the gas jet will not enter the interaction chamber. Remaining molecules in the gas jet will continue to flow until dumped out by the turbomolecular pumps in the dumping chamber.

An extra chamber can be added with a moveable gauge system installed, for measuring the gas jet density. The system includes a small cell with a hot-filament ionization gauge, into which molecules can enter through a low-conductivity channel [5] (either a hole or slit). Equilibrium pressure will be reached when the gas jet flow is equal to the effusive flow through the channel [2]. A typical measurement of the gas jet at CI, using a 0.5 mm hole, is shown in Fig. 3. With otherwise identical inlet pressure and geometrical settings for nozzle and skimmers, a monoatomic gas (e.g. neon) will have a higher density than a diatomic gas (e.g. nitrogen) because of its higher heat capacity, see Eq.1.

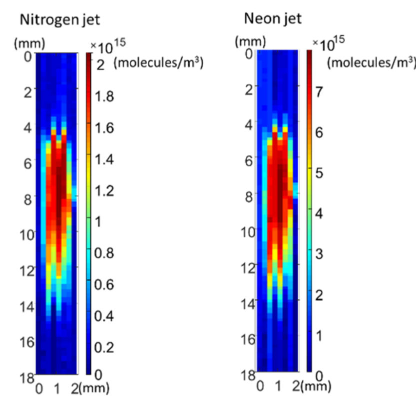

Figure 3: Jet density measurement with the system described in Fig. 2. The inlet pressure for both gases is 5 bar. The density is measured 242 mm away from the interaction point with the 3rd skimmer at a 90° angle.

From Fig. 1, the distribution of the secondaries generated from the interaction will rely intrinsically on the distribution of the primary beam. Along the x-axis it will stay the same, but along the y-axis it will blur, due to the thickness of the gas jet. On the other hand, the number of interaction events (related to the integration time) depends on the thickness of the jet, leading to a trade-off between intrinsic resolution and integration time.

GAS JET BASED IPM AND BIF

A major difference between IPM and BIF is the interaction chamber. It is more complex for IPM as the chamber needs to host the electrodes for guiding the charged particles towards the detector. As an example, the setup in CI [6-8] is shown in Fig. 4. The ions generated from the cold molecules of the gas jet will suffer less distortion from thermal movement during the collecting process compared

ISBN: 978-3-95450-208-0 doi:10.18429/JACoW-IPAC2019-WEPGW096

with residual gas based IPM in the special case of the CI installation where a low energy electron beam of 5 keV allows only for the application of a low electric field of 8.0 kV/m. Uniformity of the external field is essential for a good resolution of this method. The MCP serves as a single particle detector and converts each hit to visible light emitted by a phosphor screen. Typical images recorded by a CMOS camera from this setup with an electron beam can be seen in Fig. 5. The gas jet image and the residual gas image are separated because the ions from the gas jet possess a velocity which is normal to the collecting field and is around 780 m/s (nitrogen jet). Clearly, the residual gas image has a large distortion in the x-direction because of the thermal motion of the background gas molecules. Other gases were also tested, and their cross-section of electron impact ionisation is listed in Table 2.

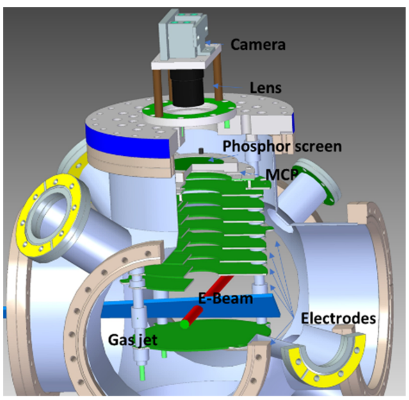

Figure 4: Interaction chamber for gas-jet based IPM beam profile monitor at CI.

Table 2: Cross Sections for Impact Ionization by 5 keV Electrons [9-11]

Process	σ (cm^2)
He^+	7.6×10^{-18}
N_2^+	1.9×10^{-17}
Ne^+	6.5×10^{-18}

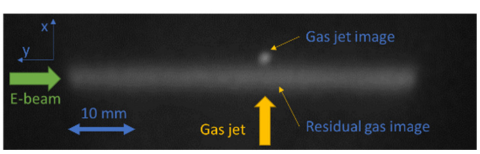

Figure 5: Image of the N2 gas-jet based IPM with a 5 keV e-beam of 10 μA. Exposure time: 120 ms, inlet pressure: 5 bar, background pressure: 2.3×10^{-8} mbar.

For the gas jet-based BIF [12], the interaction chamber is much simpler and smaller because only a viewport is needed. The imaging system may be sophisticated, including achromat lens, filter, image intensifier and CMOS camera, but the implementation is outside the vacuum chamber. Since photons are collected, the distribution won't be affected ambient electromagnetic fields in case the photons are emitted from a neutral residual gas atom. For the emission from an ion, the effect of the beam's space charge has to be taken into account as well as the fluorescence lifetime. For nitrogen molecular ions the strongest emission in the optical range has a wavelength of 391.4 nm and a lifetime of about 60 ns. For neutral neon fluorescence the strongest optical line is at a wavelength of 585.4 nm and has a 15 ns lifetime. A list of the gas species used at CI, and their properties, are shown in Table 3. Although fluorescent processes with higher cross sections exist, they are normally at UV wavelengths where non-standard optics must be used.

Table 3: Induced Fluorescence Cross Sections by 5 keV Electrons [13-15]

Emitter	λ [nm]	σ (cm^2)	τ (ns)
N_2^+	391.4	1.6×10^{-18}	60
Ne	585.4	2.7×10^{-20}	15
Ar^+	476.5	9.9×10^{-21}	9

When using BIF, one challenge is stray light; for our test setup using an electron beam, it is the radiation from the thermionic cathode and filament which has components in the spectral range of interest. These are relatively strong close to the 585.4 nm. Ne line but have a significantly lower contribution at the 391.4 nm N_2^+ line. For other cases such as the LHC, stray light could be due to synchrotron radiation. Chamber inner wall blackening must therefore be considered [16]. A profile measurement demonstrating this method at CI is shown in Fig. 6. 400 pictures with a one second exposure time had been recorded, and the fluorescence photons in each picture were then counted and added up. The background pressure was 1.6×10^{-8} mbar and the residual gas image has a lower intensity than the gas jet image. Recently, a first measurement with neon has also been performed [17] and measurements with argon gas jet is under testing.

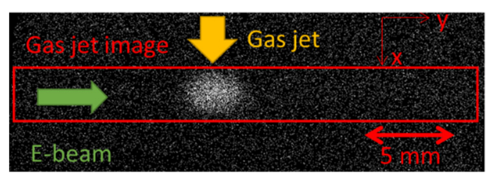

Figure 6: Image of the N_2 gas-jet based BIF monitor with a 5 keV e-beam of 0.6 mA. Integration time: 400 s, inlet pressure: 5 bar, background pressure: 1.6×10^{-8} mbar.

CONCLUSION & OUTLOOK

In this contribution, the development of supersonic gas-jet based beam profile monitors is presented. Two detection methods are compared. The discussion is based on the setup at the Cockcroft Institute, but the results can be adapted to most charged particle beams given a proper gas jet density, by modifying the nozzle-skimmer geometry and weighting the properties of the working gas.

ACKNOWLEDGEMENT

This work is supported by the HL-LHC project funded by STFC and CERN, and the STFC Cockcroft core grant No. ST/G008248/1.

ISBN: 978-3-95450-208-0 doi:10.18429/JACoW-IPAC2019-WEPGW096

REFERENCES

[1] P. Forck, "Minimal Invasive Beam Profile Monitors for High Intense Hadron Beams", in Proc. IPAC'10, Kyoto, Japan, May 2010, paper TUZMH01, pp. 1261-1265.

[2] D. R. Miller, "Free jet sources", in Atomic and Molecular Beam Methods: vol. 1, G. Scoles, Ed. Oxford University Press Inc, October 1992, pp. 14-30.

[3] M. Putignano, "Supersonic gas-Jet based beam profile monitor", Ph.D. thesis, Phys. Dept. University of Liverpool, Liverpool, UK,2012.

[4] A. Gruber, W. Bourgeois, B. Franzke, A. Kritzer and C. Treffert, "Internal gas-jet target for the ESR at GSI", Nucl. Instrum. Methods Phys. Res., Sect. A, vol. 282, pp. 87-93, 1989.

[5] H. D. Zhang, *et al.,* "3D Density Scans of a Supersonic Gas Jet for Beam Profile Monitoring", in *Proc. IBIC'16*, Barcelona, Spain, Sep. 2016, pp. 815-817.

[6] M. Putignano and C.P. Welsch, "Numerical study on the generation of a planar supersonic gas-jet", *Nucl. Instrum. Methods Phys. Res., Sect. A*, vol. 667, pp. 44-52, 2012.

[7] V. Tzoganis and C. P. Welsch, "A non-invasive beam profile monitor for charged particle beams", *Appl. Phys. Lett.*, vol. 104, p. 204104, 2014.

[8] V. Tzoganis, H. D. Zhang, A. Jeff, and C. P. Welsch, "Design and first operation of a supersonic gas jet based beam profile monitor", *Phys. Rev. Accel. Beams*, 20, p. 062801, 2017.

[9] Y. Kim, W. R. Johnson and M. E. Rudd, "Cross sections for singly differential and total ionization of helium by electron impact", *Phys. Rev. A*, vol. 61, p.034702, 2000.

[10] Z. Shen, E. Wang, M, Gong, X. Shan and X. Chen, "Electron-impact ionization cross sections for nitrogen molecule from 250 to 8000 eV", Journal of Electron Spectroscopy and Related Phenomena, vol. 225, pp. 42-48,2018.

[11] C. Chen, S, Yan, Z. Teng, Y. Wang, F.Yan and Y. Sun, "Electron-impact ionization cross sections and rates for ions of neon", *J. Phys. B: At. Mol. Opt. Phys.*, vol. 31, pp. 2667-2679, 1998.

[12] H. D. Zhang *et al*., "A Supersonic Gas Jet-Based Beam Profile Monitor Using Fluorescence for HL-LHC", in Proc. IPAC'18, Vancouver, Canada, Apr.-May 2018, pp. 1891-1894.

[13] S. Udrea *et al.,* "Preparatory Work for a Fluorescence Based Profile Monitor for an Electron Lens", in Proc. IBIC'16, Barcelona, Spain, Sep. 2016, pp. 528-531. doi:10.18429/JACoW-IBIC2016-TUPG73.

[14] S. Udrea *et al.,* "Development of a Fluorescence Based Gas Sheet Profile Monitor for Use With Electron Lenses: Optical System Design and Preparatory Experiments", in Proc. IBIC'17, Grand Rapids, MI, USA, Aug. 2017, pp. 359-363.

[15] S. Udrea and P. Forck, Milestone 1.6 report, GSI, Darmstadt, Germany, 2018.

[16] J. Glutting, "Blackening of the Interaction Chamber", BGC Collaboration Meeting at CERN, 2018. https://indico.cern.ch/event/772324/

[17] A. Salehilashkajani, *et al.,* "Commissioning of the Prototype for a New Beam Gas Curtain Profile Monitor Using Beam Induced Fluorescence for HL-LHC" presented at IPAC'19, Melbourne, Australia, May 2019, paper WEPGW093, this conference.